

Origin of dielectric relaxor behavior in PVDF-based copolymer and terpolymer films

Abhijit Pramanick, Naresh C. Osti, Niina Jalarvo, Scott T. Misture, Souleymane Omar Diallo, Eugene Mamontov, Y. Luo, Jong-Kahk Keum, and Ken Littrell

Citation: *AIP Advances* **8**, 045204 (2018); doi: 10.1063/1.5014992

View online: <https://doi.org/10.1063/1.5014992>

View Table of Contents: <http://aip.scitation.org/toc/adv/8/4>

Published by the [American Institute of Physics](#)

HAVE YOU HEARD?

Employers hiring scientists and
engineers trust

PHYSICS TODAY | JOBS

www.physicstoday.org/jobs



Origin of dielectric relaxor behavior in PVDF-based copolymer and terpolymer films

Abhijit Pramanick,^{1,a} Naresh C. Osti,^{2,b} Niina Jalarvo,^{2,3} Scott T. Mixture,⁴
Souleymane Omar Diallo,^{2,c} Eugene Mamontov,² Y. Luo,⁵
Jong-Kahk Keum,^{2,5} and Ken Littrell²

¹Department of Materials Science and Engineering, City University of Hong Kong, Kowloon, Hong Kong

²Neutron Scattering Division, Oak Ridge National Laboratory, Oak Ridge, Tennessee 37831, United States of America

³Juelich Center for Neutron Scattering (JCNS -1), Forschungszentrum Juelich, Juelich 52425, Germany

⁴Kazuo Inamori School of Engineering, Alfred University, Alfred, New York 14802, United States of America

⁵Center for Nanophase Materials Sciences, Oak Ridge National Laboratory, Oak Ridge, Tennessee 37831, United States of America

(Received 14 November 2017; accepted 20 March 2018; published online 4 April 2018)

Relaxor ferroelectrics exhibit frequency-dispersion of their dielectric permittivity peak as a function of temperature, the origin of which has been widely debated. Microscopic understanding of such behavior for polymeric ferroelectrics has presented new challenges since unlike traditional ceramic ferroelectrics, dielectric relaxation in polymers is a consequence of short-range molecular dynamics that are difficult to measure directly. Here, through careful analysis of atomic-level H-atom dynamics as determined by Quasi-elastic Neutron Scattering (QENS), we show that short-range molecular dynamics within crystalline domains cannot explain the macroscopic frequency-dispersion of dielectric properties observed in prototypical polyvinylidene-fluoride (PVDF)-based relaxor ferroelectrics. Instead, from multiscale quantitative microstructural characterization, a clear correlation between the amount of crystalline-amorphous interfaces and dielectric relaxation is observed, which indicates that such interfaces play a central role. These results provide critical insights into the role of atomic and microscopic structures towards relaxor behavior in ferroelectric polymers, which will be important for their future design. © 2018 Author(s). All article content, except where otherwise noted, is licensed under a Creative Commons Attribution (CC BY) license (<http://creativecommons.org/licenses/by/4.0/>). <https://doi.org/10.1063/1.5014992>

I. INTRODUCTION

Ferroelectrics are materials with a spontaneous electrical polarization under easily achievable conditions and are known for their extraordinary electrical, electromechanical, electro-optic and electrothermal properties. Relaxors form a special class among ferroelectrics, which are prominent for their highly disordered structures and enhanced functional properties.^{1,2} A hallmark of relaxor ferroelectrics is their peculiar dynamic properties, such as the temperature for maximum dielectric permittivity which is frequency-dependent. In addition, the peak in dielectric permittivity also extends over a broader range of temperature than normal ferroelectrics. The origin of such behavior has been widely debated. In oxide relaxor ferroelectrics, which were originally discovered fifty years ago, the origin of such frequency dispersion is explained as a result of fluctuations in nanoscale polar

^aCorresponding Author apramani@cityu.edu.hk

^bostinc@ornl.gov

^cPresent Address: Smiths Detection Inc., Edgewood, Maryland, United States of America

regions that are dispersed in a linear dielectric matrix, although the detailed physical mechanisms are still under discussion.³ In comparison, the discovery of relaxor ferroelectric polymers is rather recent, and the microscopic origins of frequency dispersion in their dielectric properties remain highly controversial.⁴⁻⁷ It needs to be noted that unlike oxides, where electrical polarization arises due to coupled ionic displacements in crystalline phases, the same arises in polymers due to a mobility of molecular dipoles along the long polymer chains in both crystalline and amorphous phases. It is then rather surprising that the broad frequency dispersions in these two separate classes of materials could be similar. Understanding the microscopic origins of dielectric frequency dispersion in polymeric materials can be a key new avenue towards a deeper understanding of the physics of relaxor ferroelectrics. From a viewpoint of materials processing, an understanding of the relative roles of different microscopic components towards the overall relaxor behavior can be important to achieve desired properties through tailored microstructures.

Relaxor-type broad frequency-dispersion of dielectric permittivity has been observed for polyvinylidene fluoride (PVDF)-based terpolymers such as PVDF-(trifluoroethylene)TrFE-(chlorofluoroethylene)CFE and PVDF-TrFE-(chlorotrifluoroethylene)CTFE, in contrast to a frequency-independent dielectric permittivity maximum in ferroelectric PVDF-TrFE copolymer near its paraelectric-ferroelectric phase transition temperature.⁶ Since their discovery, PVDF-based terpolymers have been considered for a broad array of applications including sensors and actuators, optical devices and micropumps.² Both PVDF-based copolymers and terpolymers are semi-crystalline in nature with an intermixing of crystalline lamellae and amorphous regions.

The origin of dielectric relaxation in ferroelectric polymers is not settled. In one of the earlier models, the broad frequency dispersion of dielectric permittivity in terpolymers was attributed to micro-Brownian motion of chain segments in the amorphous phase.⁸ That view was however negated in later studies, which found no correlation between dielectric losses and amorphous contents in PVDF-based copolymers and terpolymers.⁹ Instead, it was proposed that broad frequency dispersion in ferroelectric polymers with relaxor characteristics could arise from short-range molecular motion within the crystalline polar nanodomains, which are dispersed within a paraelectric matrix.⁹⁻¹¹ Nevertheless, the dielectric and ferroelectric properties of terpolymers can be altered significantly through changes in both crystal structure and microstructure,¹²⁻¹⁵ which indicates that both of these structural parameters should have important roles to play in the overall relaxor behavior. For a comprehensive understanding of the origins of relaxor behavior in polymers, it is therefore important to not only have direct measurements of molecular dynamics within crystalline domains, but also perform detailed characterization of their micro and mesostructures at different length scales. A primary reason that the comprehensive origins of relaxor behavior in polymer ferroelectrics has remained unresolved is the absence of direct measurements of molecular dynamics in microwave and radio frequency range,¹¹ and characterization of how they relate to chain arrangements. Although some insights regarding molecular dynamics are provided from first-principles calculations,¹⁶ the implications for the same are yet to be extended to understand macroscopic relaxor behavior in ferroelectric terpolymers.

Here, we report a detailed multiscale dynamic and structural characterization of PVDF-based copolymers and terpolymer films to comprehensively investigate the microstructural origins of their dielectric relaxor behavior. In order to correlate the macroscopically observed dielectric relaxation phenomenon with molecular-scale dynamic processes, we undertook direct measurements of temperature-dependent short-range H-atom dynamics with Quasi-elastic Neutron Scattering (QENS). Additionally, changes in the crystal structures of the polymer films were measured with high-temperature X-ray diffraction, which provided the physical basis for the temperature-dependent dynamic processes. The mesoscale structural features were further determined quantitatively with a variety of techniques including electron microscopy and small-angle neutron and X-ray scattering. Based on the detailed quantitative studies of atomic-level structures, molecular dynamics and mesoscale structures, we show that the short-range H-atom dynamics cannot fully explain the nature of frequency dispersion of dielectric permittivity and therefore cannot be the primary origin of relaxor behavior in PVDF-based polymers. Instead, we propose here that the molecular interactions at interfaces between the crystalline and the amorphous phases contribute significantly to the relaxor behavior in PVDF-based ferroelectric polymer films.

II. MATERIALS AND METHODS

Polymer film samples of PVDF-TrFE (45/55 molar ratio), PVDF-TrFE-CFE and PVDF-TrFE-CTFE were purchased from Piezotech, S. A. S. (France). All the polymer films were of thickness 40 μm , and were characterized in their as-obtained unpoled condition. The technical parameters are available from the supplier's website (<http://www.piezotech.eu/en/Products/Devices/>) and in earlier reviews.^{2,6}

For dielectric permittivity measurements, the polymer films were coated with gold electrodes and contacted with electrical wires for dielectric measurements. The dielectric properties were measured in the frequency range from 100 Hz to 100 kHz using an Agilent 4284 A Precision LCR meter. All measurements were taken using an AC test voltage of 100 mV, while heating up from 200 K to 370 K.

For a direct measurement of molecular scale dynamics, QENS measurements were obtained from the polymer films using the backscattering spectrometer BASIS at the Spallation Neutron Source (SNS).¹⁷⁻²⁰ The measurements were taken in the temperature range between 300 K and 370 K, where the microscopic dynamics of H atomic motions in the polymer samples becomes clearly observable within the spectrometer window. This is also the temperature range over which a frequency dispersion of the dielectric permittivity peak is observed at higher frequencies above 100 kHz. Data reduction was done by using the Mantid package,²¹ and data analysis was carried out with DAVE software.²² Details about the measurement procedure are provided in the [supplementary material](#).

For characterization of molecular and crystal structures, we employed Fourier Transform Infrared (FTIR) Spectroscopy and X-ray diffraction, respectively. Finally, quantitative characterization of the microstructural features of the polymer films were obtained with a combination of microscopy and scattering techniques. Scanning Electron Micrographs of cross-sections of the polymer films were obtained using JEOL JSM-6335F field-emission Scanning Electron Microscope (SEM). The cross-sections of the films were prepared carefully by cryo-fracture in a liquid nitrogen atmosphere. Furthermore, small angle X-ray and neutron scattering (SAXS/SANS) were used to quantitatively characterize the microstructural parameters observed from SEM, such as amorphous/crystalline volume fractions and the length scales of the crystalline and amorphous domains. Experimental details for all these measurements are provided in the [supplementary material](#).

III. RESULTS AND DISCUSSION

A. Frequency dispersion of dielectric permittivity

Figure 1 a, b, c show frequency and temperature-dependent spectra of real component (ϵ') of the dielectric permittivity and loss ($\tan\delta$) spectra of the copolymer PVDF-TrFE and the terpolymer PVDF-TrFE-CFE and PVDF-TrFE-CTFE films. In all of those films, two main features in their dielectric spectra can be identified. The first feature is prominent between 250 K and 300 K, which is stronger in terpolymers than in the copolymer. In earlier studies, this part of the spectra was attributed to the amorphous phase.⁹ The second feature is observed between 300 K and 350 K, which is in general sharper than the feature at lower temperatures for all the samples. The different temperature regimes become clearer from the loss spectra. Here, the first feature shows a dispersive nature and progressively shifts to higher temperature with increasing frequencies. The second feature at higher temperatures show dispersive behavior for frequencies beyond 100 kHz.

There are several features in the ϵ' and $\tan\delta$ spectra, which are intriguing. Note that, for the terpolymer films, while the shoulders from the lower temperature feature in ϵ' and $\tan\delta$ spectra are distinctly observed between 250 K and 300 K at lower frequencies, a merging of the two features occurs for frequencies greater than 100 kHz and the overall peak in dielectric permittivity is located above 300 K. A sharp decrease in peak value for ϵ' for terpolymers is also observed for frequencies greater than 100 kHz. In comparison, those two features in the ϵ' and $\tan\delta$ spectra remain distinct for the PVDF-TrFE copolymer film and the peak for ϵ' does not exhibit a sharp reduction at higher frequencies.

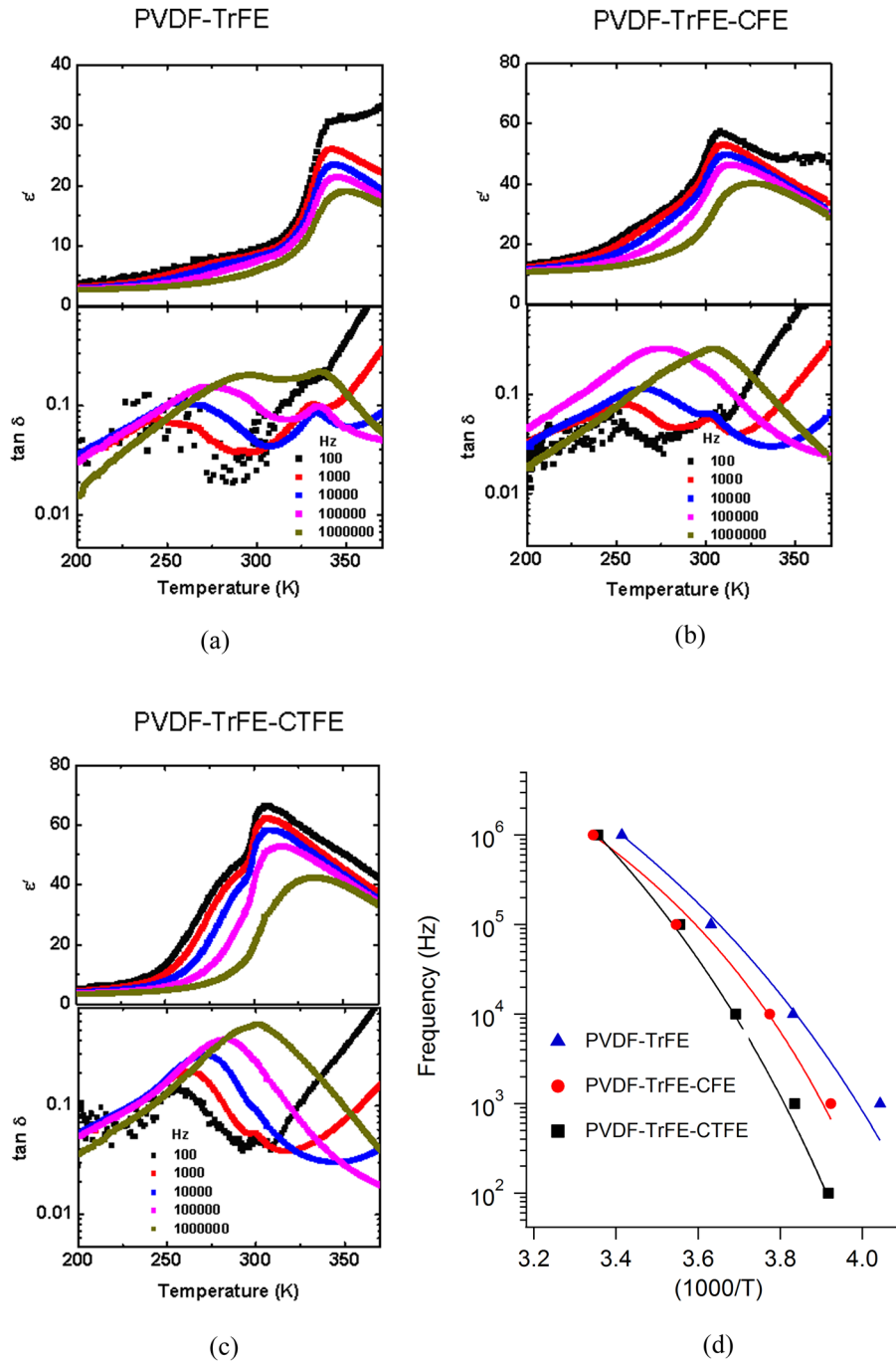


FIG. 1. Frequency dispersion of dielectric permittivity. (a-c) Real (ϵ') components of the dielectric permittivity and loss ($\tan \delta$) of copolymer PVDF-TrFE and terpolymers PVDF-TrFE-CFE and PVDF-TrFE-CTFE, as functions of temperature and probing frequency. (d) Fits for T_m corresponding to the maxima in the dispersive component of $\tan \delta$ with respect to frequency, following Vogel-Fulcher relation as shown in Equation (1).

If we associate the features at lower and higher temperatures to different microstructural domains, then we can infer that their relative contributions to the overall broad dispersion of dielectric permittivity are different in copolymers and terpolymers. However, an exact understanding of this issue is not yet clear.^{4-6,9} A clearer insight into the origins of relaxor behavior can be obtained by investigating the energetics of the respective dominant relaxation processes.

A broad dispersion of macroscopic dielectric permittivity, which was observed at the lower temperatures regime, is a signature of a distribution of relaxation times for microscopic phenomena. In order to gain insights into these relaxation process, the dielectric data was fitted to obtain the respective temperatures T_m for maxima in the loss spectra. Due to the inherent broadness of the peaks, either one or two Pearson VII peak profile functions were used to fit the spectra (see [supplementary material](#)). We used the Vogel-Fulcher relation⁵ to equate the temperature T_m corresponding to the maxima in $\tan\delta$ at lower temperatures with respect to the inverse of relaxation time $1/\tau$:

$$\frac{1}{\tau} = \omega_0 \exp\left(-\frac{E_{a(d)}}{k_B (T_m - T_f)}\right) \quad (1)$$

where ω_0 is the hopping frequency, $E_{a(d)}$ is the activation energy for the dominant relaxation mechanism, k_B is the Boltzmann constant, T_m is the temperature corresponding to maxima in loss ($\tan\delta$) and T_f corresponds to the freezing temperature of the microscopic relaxation phenomena. The fittings are shown in Figure 1 d and the fit parameters are listed in Table I. The maximum $E_{a(d)}$ is observed for the PVDF-TrFE-CTFE film.

Relaxation of molecular chains in the amorphous phase has been proposed earlier as a possible origin of relaxor behavior in polymer ferroelectrics.^{5,11} However, as also noted earlier in Refs. 9 and 10, T_g in all the films is ~ 200 K, which is 50 K lower than the first peak in the dielectric permittivity spectra at ~ 250 K. This therefore suggests that the relaxation within the amorphous domains cannot entirely account for the frequency dispersion of the dielectric permittivity. Another possibility is that such dielectric dispersion is mainly due to the short-range molecular motion within the crystalline domains.⁹⁻¹¹ However, this view can be negated by taking a careful look at $E_{a(d)}$. It can be seen that $E_{a(d)}$ for both terpolymers is higher than $E_{a(d)}$ in the copolymer. Indeed, $E_{a(d)}$ is highest for PVDF-TrFE-CTFE which has a much bulkier termonomer, similar to an earlier report.⁷ If molecular motion within crystalline domains were the dominating contributor to the frequency dispersion of dielectric maxima as shown in Figure 1, this would counterintuitively suggest that the molecular dynamics within the crystalline domains becomes more hindered with the introduction of termonomers. Therefore, in order to reconcile the macroscopic dielectric dispersion with microscopic phenomena, a closer scrutiny of the molecular motion is necessary. For this purpose, we undertook direct measurement of microscopic molecular dynamics using QENS, as described below.

B. Quasielastic neutron scattering

The QENS data, which are measured in the energy transfer space, are related to the decay of the particle spatial correlation in the temporal space through Fourier transformation. In this case, we can assume a dispersion of the dielectric permittivity peak in the polymer films is related to the temporal correlations among the microscopic electrical dipoles, which are further correlated to the short-range H-atoms motions along the polymer chains. The spatial correlation decay of the H-atoms over short-ranges can be very well characterized using QENS. Therefore, QENS is an excellent technique for a direct characterization of molecular scale relaxational dynamics in ferroelectric polymers in the ns-to-ps timescales,¹⁷⁻¹⁹ which could then be compared to and possibly reconciled with macroscopic dielectric relaxor behavior.

For each sample, the elastic incoherent neutron scattering (EINS) contribution was extracted from the full spectra by integrating the elastic peak. A quantity of interest, the average mean-square-displacement (noted MSD or $\langle u^2 \rangle$), can be obtained by using a Gaussian approximation

TABLE I. Activation energy for the dominant relaxation process as obtained from fitting of frequency-dispersion of dielectric permittivity.

Polymers	Activation Energy (kJ mol ⁻¹)
PVDF-TrFE	9.64
PVDF-TrFE-CFE	10.48
PVDF-TrFE-CTFE	10.85

$S_{el}(Q) = A \times e^{-Q^2 \langle u^2 \rangle / 3}$. We observed a rapid increase in MSDs at ~ 290 K (Figure S1 of the [supplementary material](#)) for all samples, suggesting the onset of the H-atom mobility at this temperature.

In order to capture the detailed microscopic dynamics, we collected QENS spectra at four different temperatures between 300 K and 370 K. The highest temperature measured (370 K) is well below the melting temperature, therefore the current study is limited to molecular dynamics within the solid state. A broadening of the QENS spectra for all the polymer films can be clearly noted, as shown in Figure 2 a, b, c. An increase in peak broadening with temperature implies that localized relaxational motions of H-atoms are involved in both the copolymer and the terpolymer films. Below, we provide a detailed analysis of the QENS spectra to gain insights into the length and timescales of localized motion of H-atoms, which could provide a direct window into the molecular processes responsible for relaxor behavior in the ferroelectric polymer films.

The measured QENS spectra were fitted independently at each wavevector, or $|\vec{Q}|$ value, using the following expression:

$$I(Q, E) = [p_1(Q) \delta(E) + (1 - p_1(Q)) S(Q, E)] \otimes R(Q, E) + B(Q, E) \quad (2)$$

where $\delta(E)$ is a Dirac delta function and $p_1(Q)$ is the Elastic Incoherent Structure Factor (EISF). In the above equation, the factor $p_1(Q)$ represents the elastic scattering fraction and $(1 - p_1(Q))$ represents the

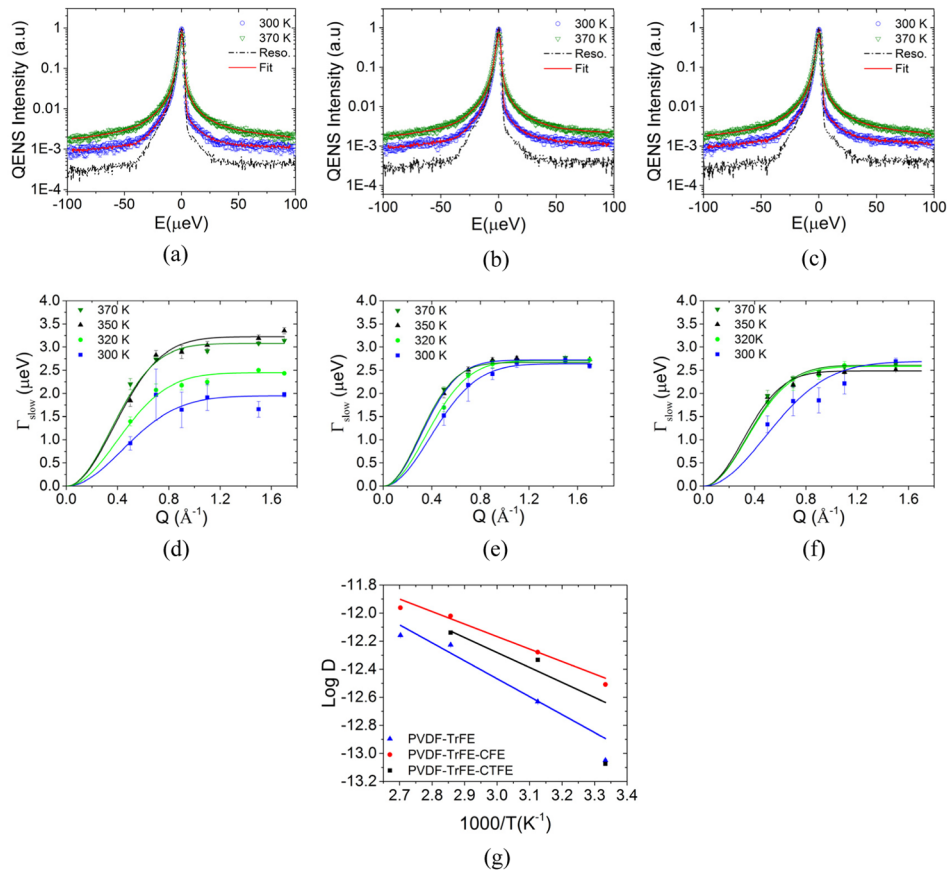


FIG. 2. Microscopic dynamics of relaxation-type H atomic motion. (a)-(c) QENS spectra of the polymers at a representative $Q = 0.9 \text{ \AA}^{-1}$ (a) PVDF-TrFE (b) PVDF-TrFE-CFE (c) PVDF-TrFE-CTFE. Symbols correspond to the experimental data, dotted lines represent the instrumental resolution measured at 20 K for each sample, and the solid lines are the fits obtained using the model functions (Eq. 2) described in the text. (d)-(f) HWHM of a Lorentzian representing the slow component on the model fitted to the QENS spectra as a function of Q^2 for (d) PVDF-TrFE (e) PVDF-TrFE-CFE (f) PVDF-TrFE-CTFE. The solid lines are fits of Eq. 5 as described in the text. (g) Temperature dependence of short-range jump diffusivity coefficient D for the relaxational atomic motions, calculated following Arrhenius behavior below 370 K.

spectral weight of the QENS components within the total scattering intensity. A linear background term, $B(Q, E)$, is added to fit the dynamic structure factor, $S(Q, E)$, after convolution with instrumental resolution, $R(Q, E)$. The temperature dependences of EISF for all the films are shown in Figure S1 in the [supplementary material](#).

The details of the *length scales* of the relaxational motion of H-atoms can be obtained by fitting the $p_1(Q)$ component, or Elastic Incoherent Structure Factor, EISF, with the following expression:

$$p_1(Q) = C + (1 - C)j_0^2\left(\frac{QL}{2}\right) \quad (3)$$

where $j_0(x)$ is the zeroth spherical Bessel function of first kind. $(1 - C)$ is the fraction of protons undergoing short-range diffusion with a cylinder of length L , whereas the fraction C accounts for the protons immobile on the resolution scale of the measurement.^{19,20} Here L corresponds to the distance along the polymer backbone over which protons can move easily. The parameters extracted using Equation (3) are presented in Table II. We found similar fractions of mobile protons for both the copolymer and the terpolymers at 300 K, consistent with earlier observations in PVDF and PVDF-TrFE.¹⁹ However, L is larger in terpolymers as compared to the copolymer, which can be attributed to a decrease in inter-chain interaction caused by the introduction of the termonomers (CEF and CTFE) (see Section III C). Increase in L is more pronounced for PVDF-TrFE-CTFE because of the much bulkier termonomer (CTFE). In general, an increase in $(1 - C)$ with temperature can also be expected as a result of increasing the fraction of mobile protons in both the crystalline and amorphous domains.¹⁷ A larger increase in L and $(1 - C)$ for PVDF-TrFE copolymer film on increasing the temperature from 300 K to 350 K, as compared to terpolymers, can be attributed to a clear ferroelectric-paraelectric phase transition in this case, as revealed from X-ray diffraction measurements (see Section III C) and also from DSC measurements (Figure S2 of the [supplementary material](#)). However, no clear ferro-to-paraelectric transition could be observed from structural measurements in the terpolymer films in this temperature range, and therefore changes in L and $(1 - C)$ are less apparent. At 370 K, all the polymer samples have roughly the same fraction of mobile protons within a comparable length, since they are closer to their melting transitions.

In order to characterize the *time scales* of the relaxational motion of the H-atoms, $S(Q, E)$ in Equation (2) was further modeled as a sum of two Lorentzians, one accounting for a slower dynamical process, especially associated with short range molecular motion within the crystalline domains, and another capturing much faster process, likely originating from the amorphous region (or interfaces between crystalline and amorphous domains), as follows:

$$S(Q, E) = p_2(Q) \frac{1}{\pi} \frac{\Gamma_1(Q)}{\Gamma_1^2(Q) + E^2} + (1 - p_2(Q)) \frac{1}{\pi} \frac{\Gamma_2(Q)}{\Gamma_2^2(Q) + E^2} \quad (4)$$

Here $p_2(Q)$ and $(1 - p_2(Q))$ are relative weights of first and second Lorentzians with half width at half maximum (HWHM), $\Gamma_1(Q)$ and $\Gamma_2(Q)$, respectively. The effect of temperature on the HWHM corresponding to the slow components, $\Gamma_2(Q)$, is presented in Figure 2 d, e, f. A strong Q-dependence of $\Gamma_2(Q)$ at all measured temperatures confirms the presence of a translational (on the length scale probed) motion of H-atoms in all the samples. This relationship, in fact, shows an increase in broadening with Q at low Q values, and becomes flat at higher Q's, suggesting a jump type dynamic process involving protons. Therefore, as in the previous study in a similar system,¹⁹ $\Gamma_2(Q)$ was

TABLE II. Characteristics of lengthscales of relaxational H atom dynamics as obtained from fitting of EISF using Equation (3).

Polymers		300 K	320 K	350 K	370 K
PVDF-TrFE	(1-c)	0.21 ± 0.02	0.58 ± 0.01	0.68 ± 0.01	0.73 ± 0.01
	L (Å)	2.41 ± 0.27	3.08 ± 0.09	3.23 ± 0.17	3.13 ± 0.05
PVDF-TrFE-CEF	(1-c)	0.19 ± 0.01	0.37 ± 0.02	0.65 ± 0.03	0.80 ± 0.02
	L (Å)	2.89 ± 0.16	2.87 ± 0.16	2.91 ± 0.13	3.21 ± 0.10
PVDF-TrFE-CTFE	(1-c)	0.18 ± 0.00	0.37 ± 0.01	0.70 ± 0.01	0.84 ± 0.00
	L (Å)	3.16 ± 0.16	2.86 ± 0.15	2.86 ± 0.07	3.11 ± 0.03

analyzed using a jump diffusion model involving a Gaussian distribution of jump lengths, which is expressed as:

$$\Gamma_2(Q) = \frac{1}{\tau} \left[1 - \exp\left(-\frac{Q^2 r_0^2}{2}\right) \right] \quad (5)$$

where τ and r_0 are the characteristic time and the average length of jumps, respectively. Here, it must be clarified that many dynamic processes in polymers measured with QENS are customarily described in terms of localized diffusivity of moving particles, yet from the macroscopic perspective they can be seen as relaxations of side groups, as long as the polymer remains in the solid state. Note that $\Gamma_1(Q)$, which represents the fast component, did not show any specific trend with Q , and therefore suggests some very fast and more localized dynamic process, possibly within the amorphous region (see [supplementary material](#)). The assignment of the fast dynamics to amorphous regions is corroborated by the amorphous volume fraction in the polymer films. The average relative weight of the fast component, $p_2(Q)$, extracted from the model fit is $\sim 25\%$, which is consistent with the amorphous volume fraction obtained from SAXS (See Table V).

From the analysis of $\Gamma_2(Q)$ based on Equation (5), the characteristic residence times (τ) and the average jump lengths (r_0) for the slower atomic relaxation process were then extracted. The results are presented in Table III. In general, τ is smaller for the terpolymers than the copolymer, especially below the ferroelectric-paraelectric phase transition of the copolymer. This can be attributed to an increase in the volume of unit cell by the presence of bulkier CFE and CTFE monomers that promotes a faster mobility of protons. When temperature is increased, τ drops for copolymer PVDF-TrFE up to the phase transition temperature (~ 330 K), beyond which it becomes roughly constant. This observation indicates that below the ferroelectric-paraelectric phase transition temperature of the copolymer, τ remains roughly the same for both copolymer and terpolymers. Finally, we note that despite the differences in their bulkiness, PVDF-TrFE-CFE and PVDF-TrFE-CTFE both have comparable τ within the investigated temperatures. With regard to the average jump length or r_0 , they rise with increasing temperature for all the samples. Also, r_0 is generally higher for terpolymers than the copolymer. One exception is that we observe a slightly lower value of r_0 for PVDF-TrFE-CTFE at 300 K as compared to other samples, which could be associated with the presence of a defective ferroelectric phase (see Section III C). Also for PVDF-TrFE-CTFE at 370 K, there is a decrease in r_0 , which likely is due to the lower melting point of this polymer as evident from DSC thermograms (Figure S2 of the [supplementary material](#)).

Considering both τ and r_0 , we next calculated the short-range jump diffusivity coefficient ($D = r_0^2/2\tau$, as the dimensionality of this process is determined by Eq. 3 and Eq. 5) for the relaxational H atomic motions in the different polymer films. The results are shown in Table IV and Figure 2 g.

TABLE III. Characteristics of timescales of relaxational H atom dynamics as obtained from fitting of the HWHM of the slow component using Equation (4).

Polymers		300 K	320 K	350 K	370 K
PVDF-TrFE	τ (ps)	124.0 \pm 3.2	98.72 \pm 1.1	75.95 \pm 1.6	78.53 \pm 1.0
	r_0 (Å)	2.31 \pm 0.23	2.54 \pm 0.17	2.71 \pm 0.17	2.87 \pm 0.27
PVDF-TrFE-CFE	τ (ps)	91.5 \pm 1.1	98.1 \pm 0.4	88.8 \pm 0.4	90.5 \pm 1.3
	r_0 (Å)	2.60 \pm 0.18	2.88 \pm 0.04	3.27 \pm 0.13	3.40 \pm 0.28
PVDF-TrFE-CTFE	τ (ps)	86.0 \pm 2.3	90.9 \pm 1.7	96.3 \pm 0.8	91.4 \pm 0.9
	r_0 (Å)	1.90 \pm 0.21	2.83 \pm 0.21	3.21 \pm 0.16	2.89 \pm 0.17

TABLE IV. Activation energy $E_{a(m)}$ for short-range relaxation-type H atomic motion obtained from QENS.

Polymers	Activation Energy (kJ mol ⁻¹)
PVDF-TrFE	10.63 \pm 2.07
PVDF-TrFE-CFE	7.40 \pm 0.71
PVDF-TrFE-CTFE	8.86 \pm 5.03

Overall, it is clear that the introduction of bulkier groups enhances D in terpolymers as compared to the copolymer, which translates to easier short-range molecular motion in the terpolymers. It can also be observed that changes in D are mainly a result of changes in atomic jump lengths r_o . This provides an avenue to establish a clear connection between molecular relaxational motions and the crystallographic lattice spacings for the polymer chains, which is further investigated in the Section III C.

Below we explore correlation between frequency dispersion of the dielectric permittivity and the microscopic molecular relaxational dynamics by comparing the activation energies of the respective phenomena. For this, we calculated the activation energy ($E_{a(m)}$) for short-range relaxational motion from the Arrhenius fit of the temperature dependence of D . The results are shown in Figure 2 c and the parameters of the fit are summarized in Table IV. To the best of our knowledge, these are the first direct measurements of the energetics of short-range molecular dynamics in PVDF-based ferroelectric terpolymers. The $E_{a(m)}$ for PVDF-TrFE-CTFE has a slightly larger error bar; we attribute this to the presence of a mixture of defective ferroelectric and paraelectric domains at 300 K, which leads to anomalous decrease in jump diffusivity D .¹⁹ In general, $E_{a(m)}$ for molecular dynamics is larger in the copolymer as compared to terpolymers. In Figure 2 g, the slope of the line is maximum for the film PVDF-TrFE, which is reflected in maximum $E_{a(m)}$ for this composition. This clarifies that indeed the short-range molecular motion should require lower activation energy in terpolymers as compared to the copolymer.

Nevertheless, the trend for $E_{a(m)}$ or the short-range relaxational motion of atoms as obtained directly from QENS are inconsistent with that of $E_{a(d)}$ that was determined from dielectric permittivity measurements. That is, while $E_{a(d)}$ or the activation energy for the dominant microscopic relaxation process is predicted to be smaller in the copolymer from dielectric permittivity measurements, the $E_{a(m)}$ for short-range molecular motion within the crystalline domains is in fact larger in the copolymer. In addition, it can also be observed that the peak frequencies for dielectric permittivities are higher for the copolymer than the terpolymers, whereas this trend is reversed for the short-range jump diffusivity coefficient D . Please note that D here refers directly and exclusively to the dynamics of molecular motion within the crystalline domains, and does not reflect the longer lengthscale microstructural interactions. In view of this, we can conclude that the dynamics of short-range molecular motion within crystalline domains cannot be the principal origin of macroscopic dielectric dispersion observed in ferroelectric terpolymers.

Therefore, in order to reconcile the characteristics of dynamics observed at the macroscopic and the atomic scales, we next undertook a detailed structural analysis of the copolymer and the terpolymer samples at different length-scales, as presented below.

C. Molecular and crystallographic structural characterization

To clarify the role of crystal structures on the overall dynamics, high-temperature X-ray diffraction experiments were conducted on all the polymer films. The temperature dependent diffraction patterns are shown in Figure 3 a, b, c. The 2θ values are converted to corresponding d -spacings using Bragg's law and plotted in Figure 3 d, e. For the PVDF-TrFE film, two set of reflections are observed in the X-ray diffraction patterns. The first set of reflections are centered around higher 2θ values at $\sim 18.9^\circ$ in the unpoled film, which are attributed to the (200/110) reflections of the ferroelectric phases β and a defective ferroelectric phase (γ).^{13,23–25} This is consistent with the FTIR spectra measured at room temperature (RT), which shows a dominance of the $T_{m>4}$ (all-trans) and the TTTG (trans-trans-trans-gauche) bands over the TG (trans-gauche) band (Figure 3 g).¹⁵ With increasing temperature, the ferroelectric phases gradually transform into the paraelectric phase α , which is evident from shifting of the same (200/110) reflections to a lower 2θ of $\sim 18^\circ$.²⁶

The PVDF-TrFE-CTFE film shows a very broad diffraction peak at RT, centered at $\sim 18.2^\circ$, which is attributed to (200/110) reflections from a defective ferroelectric relaxor phase (γ) and the α phase. This is again evident from the FTIR spectra, which shows a dominance of the TTTG and the TG FTIR bands over the $T_{m>4}$ peak. With increasing temperature, the XRD peak becomes sharper and moves to lower 2θ values as a result of thermal expansion of the lattice. There is a slight change in the slope of the d -spacings versus temperature plot, which can be attributed to a defective

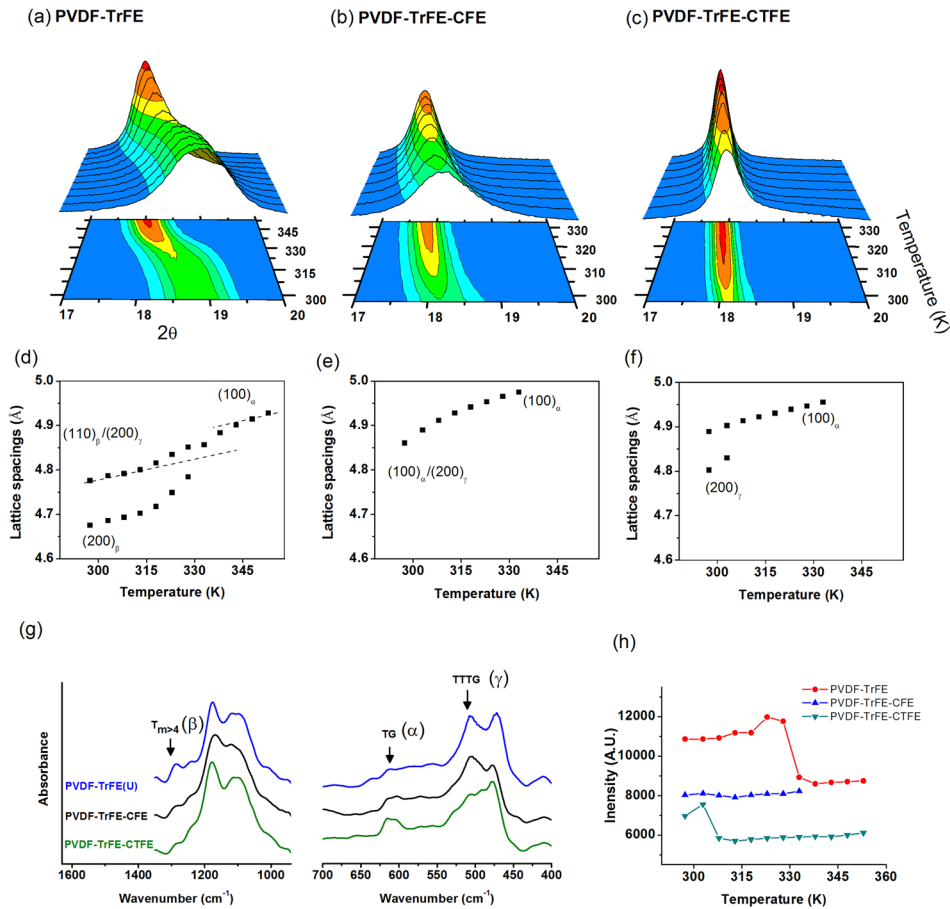


FIG. 3. Atomic-scale and crystal structures of copolymer and terpolymer. (a)-(c) High-temperature X-ray diffraction patterns from the different polymer films showing evolution of crystalline phases as function of temperature. (d)-(f) Evolution of lattice parameters as function of temperature, which was obtained from fitting of the X-ray diffraction peaks shown in (a)-(c). (g) FTIR spectra from the different polymer films, which inform about the molecular configurations corresponding to the different crystalline phases present at room temperature. (h) The temperatures corresponding to the structural phase transition temperatures can be clearly observed from the variation in total integrated intensities of diffraction peaks shown in (a)-(c).

ferroelectric-to-paraelectric phase transition,²⁶ although the peaks from the two different phases could not be clearly distinguished due to their very broad nature.

The diffraction pattern from the PVDF-TrFE-CTFE film is interesting as it shows a sharp peak at $\sim 18.1^\circ$ and a broad shoulder at $\sim 18.5^\circ$ at RT. The former is attributed to the paraelectric α phase, which correlates with the dominance of the TG band in the FTIR spectrum. The broad shoulder at $\sim 18.5^\circ$ is attributed to a highly defective ferroelectric relaxor phase (γ).^{13,23-25} This is supported from a broad intensity distribution in the region of the TTTG band in the FTIR spectrum. With increasing temperature, the peak from the ferroelectric relaxor phase decreases leading to only the paraelectric α phase at higher temperatures. The ferro-to-paraelectric phase transition can also be observed from sharp change in integrated peak intensity, as shown in Figure 2 h.

The temperature-dependent crystallographic parameters provide the physical basis for interpreting the short-range relaxational dynamics of H atom motion measured directly with QENS. The results validate the earlier hypothesis that increased short-range dynamics of H-atoms along the chain dimension correlates with an increase in crystallographic lattice parameter, which is furthermore defined by the chain spacings.^{16,26} In other words, a lower $E_{a(m)}$ related to relaxational atomic motions in the terpolymer films can be understood based on the fact that the interchain distances are larger in terpolymers and there are fewer interchain interactions.²⁷ Furthermore, there is a significant increase in H-atom dynamics over the course of the ferroelectric-to-paraelectric

phase transition, which is due to a jump in lattice volume over the same temperature range. These results unambiguously establish the physical justifications for enhanced molecular dynamics with lower activation energies in terpolymers as compared to the copolymer. Nevertheless, this is in contrast with findings from dielectric permittivity measurements, which instead indicated that the dominant relaxation mechanism should have lower activation energy in the copolymer film. It therefore reinforces the notion that short-range molecular dynamics within the crystalline domains cannot be the dominant mechanism for frequency-dispersion of macroscopic dielectric permittivity.

D. Microstructural characterization

Since we determined from the above discussion that short-range relaxational motion of atoms is not the dominant contributor to frequency dispersion of dielectric permittivity, we further investigated the effects of the other microstructural features on overall relaxational dynamics. The microstructural features were first qualitatively identified from SEM micrographs. The quantitative details for all the microstructural parameters were subsequently determined from X-ray and neutron scattering measurements.

Figure 4 shows the scanning electron micrographs of the cross-sections of the different polymer films. All the films contain a dispersion of disc-shaped particles in an amorphous matrix. From a visual comparison, the particle sizes seem smaller in the terpolymers as compared to the copolymer and is smallest for PVDF-TrFE-CTFE film.

A quantitative characterization of crystallite sizes in the different polymer films is obtained from analysis of the X-ray diffraction peaks using the Scherrer equation,

$$B = \frac{0.9\lambda}{t \cos \theta} \quad (6)$$

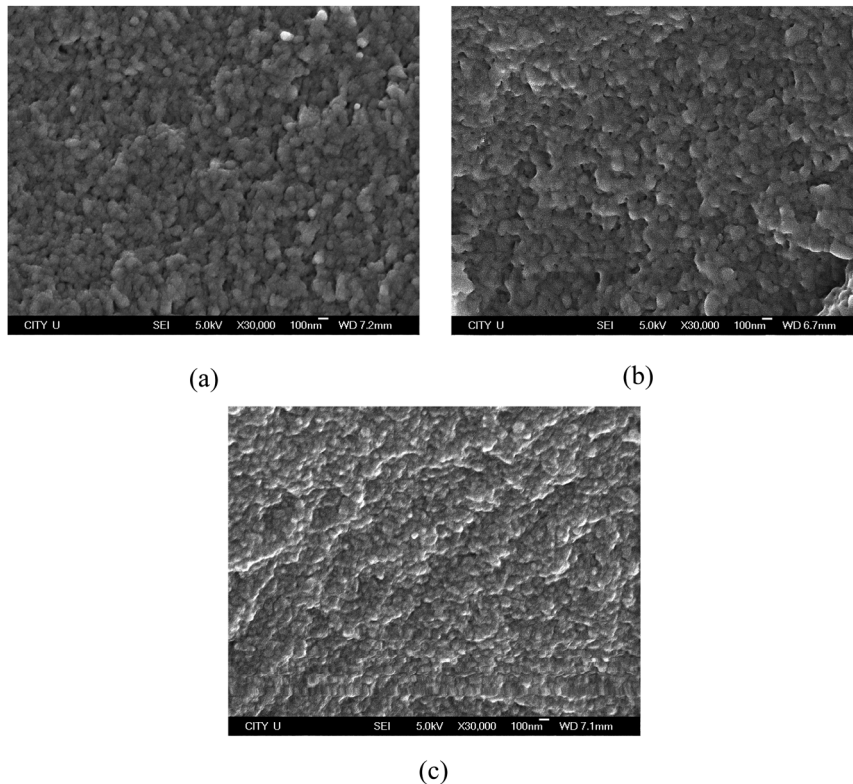


FIG. 4. Scanning electron micrographs of cross-sections of the different polymer films showing clear changes in particle sizes: (a) PVDF-TrFE (b) PVDF-TrFE-CFE (c) PVDF-TrFE-CTFE. Quantitative microstructural characterizations are furthermore provided from analysis of peak-widths of X-ray diffraction peaks and small-angle X-ray scattering.

TABLE V. The details of the lamellar morphology of the copolymer and terpolymer films, such as lamellar correlation length (L), crystalline lamellar thickness (L_c), amorphous layer thickness (L_a), and crystal volume fraction (v_c) as evaluated from SAXS data using one-dimensional correlation function (CF(r)). Lamellar correlation length (L_{SANS}) was obtained from the maximum peak position of the SANS curves. The crystalline domain size (L_{cx}) as determined from X-ray diffraction peak-width analysis.

	PVDF-TrFE	PVDF-TrFE-CFE	PVDF-TrFE-CTFE
L (Å)	385	300	277
L_a (Å)	56.0	49.0	68.0
L_c (Å)	329	251	209
L_{SANS} (Å)	363	288	285
L_{cx} (Å)	313 (β)	200 (α/γ)	230 (α)/90(γ) ^a
V_c	0.85	0.84	0.75

^a γ refers to the defective ferroelectric phase in the relaxor terpolymers.

where B is the FWHM of the Bragg diffraction peak which appears at scattering angle 2θ , λ is the X-ray wavelength and t is the average crystallite size. Quantitative values for the lengthscales of the crystalline and amorphous domains as well as the volume fractions of the crystalline phases, are also obtained from the analysis of the SAXS and SANS measurements (see [supplementary material](#)). All the results for microstructural analyses appear in Table V.

It can be observed that the crystalline domain sizes in terpolymer films are consistently lower than what is observed for the copolymer film. In general, the crystallite sizes vary between 25-30 nm, which is also observed from the SEM micrographs. This confirms that the microscopic domains observed in the SEM images are crystalline in nature. Interestingly, for the PVDF-TrFE-CTFE film, we find a bimodal distribution with average crystallite sizes of ~ 25 nm and ~ 10 nm. The latter could be identified as defective ferroelectric nanodomains, which are dispersed in between the larger paraelectric crystalline domains. As the crystalline particle sizes become smaller in an amorphous matrix, and provided that the crystalline phase fraction remains roughly similar, the contact area at interface between the crystalline domains and the amorphous matrix should increase. This can be clarified from a simple illustration such as shown in Figure 5 a. Table V lists the correlation length for the crystalline (L_c) and the amorphous (L_a) components within each particle, which were

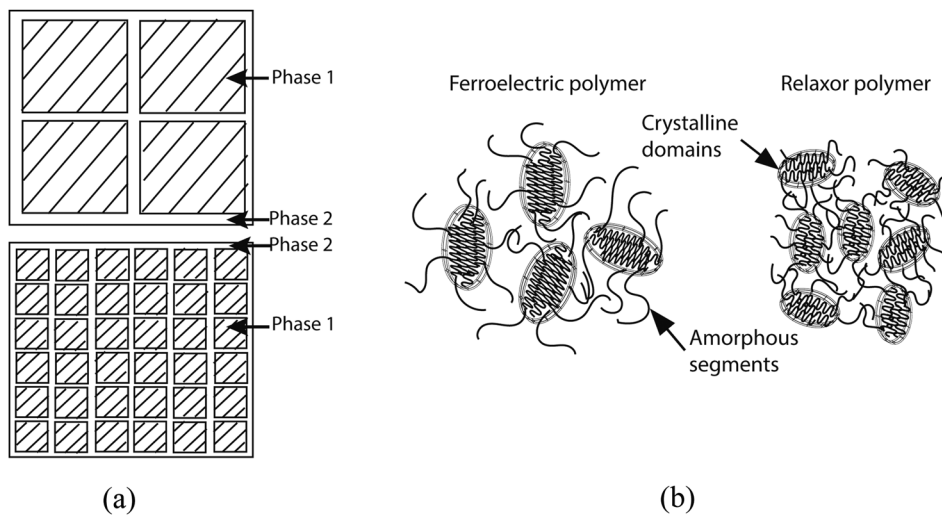


FIG. 5. Illustration of change in microstructural characteristics of normal and relaxor ferroelectric polymer films, respectively. (a) The interfacial contact area between the crystalline Phase 1 and the amorphous Phase 2 is increased as the domain size for Phase 1 is decreased, provided the volume fractions of two phases are comparable in two cases. (b) In polymer with relaxor ferroelectric properties, the crystalline domains are shortened with consequent increase in crystalline-amorphous interfaces. The molecular chains have a larger likelihood of getting tangled up at interfaces for smaller particle sizes.

obtained from analysis of X-ray scattering patterns. The relative proportion of the interfacial contact area for disc-shaped particles could be estimated as proportional to $L_c/(L_c + L_a)^2$. Based on values shown in Table V, this parameter is $\sim 25\%$ more for terpolymers as compared to the copolymer. Therefore, it is apparent that the crystalline-amorphous interfacial area increases on going from the copolymer to the terpolymer films. Consequently, taking into account of the information shown in Figure 1, a proportional correlation can be observed between the extent of crystalline-amorphous interfaces, the relative strength of the dispersive component of ϵ' between 250 K and 300 K and $E_{a(d)}$ for the dominant relaxational processes as predicted from dielectric permittivity measurements.

IV. CONCLUSIONS

Taking a holistic view, we summarize the main findings of this study as follows. First, from dielectric permittivity measurements of PVDF-based copolymer and terpolymer films, we found that the dominating microscopic relaxational mechanism in terpolymers have higher activation energies than those in the copolymer. Second, based on direct measurements of short-range relaxational motion of H atoms using QENS and supporting physical justification from XRD and FTIR, we concluded that the relaxor behavior in terpolymers cannot be explained on the basis of short-range molecular dynamics within the crystalline domains. Finally, from microstructural analysis, we observe a proportional correlation between the amount of crystalline-amorphous interfaces and the strength of the frequency-dispersive component of ϵ' . From this viewpoint, we propose a new mechanism for the origin of relaxor behavior in polymer ferroelectrics.

The broad dispersion in dielectric permittivity, as a hallmark of relaxor behavior, originates from microscopic dynamics which occur at the interfacial region between the crystalline and the amorphous phases. As the size of the particles decrease and the crystalline-amorphous interfacial area increase, the amorphous chain segments at the edge of the particles not only have a greater chance to get entangled with the crystalline lamellae but also with the amorphous chain segments from the neighboring particles. This is illustrated in Figure 5 b. The entangled chain segments in the amorphous matrix, as compared to those within the crystalline lamellae, are much more flexible in responding to an electric field. Their entangled nature ensures that the neighboring crystalline domains now exhibit an increased “exchange coupling” effect, leading to a greater dielectric response. It can also be expected that as the amorphous chain segments from the neighboring domains becomes more entangled, the activation energy for their dynamics will naturally increase, which can explain the correlation between the interfacial area fraction and $E_{a(d)}$. The interfacial microscopic dynamics between crystalline and amorphous domains likely have critical dynamics in the MHz regime, which is reflected by a sharp departure of dielectric permittivity spectra for terpolymers at this frequency (Figure 1).

The mechanism described above is generally attuned to other recent studies in oxide ferroelectrics, where the interactions between the different components of a microstructure are found to be more important than individual components themselves in determining the overall material response.^{28,29} We also note that in a recent study on PVDF-TrFE copolymer films, the interactions between the amorphous and crystalline regions are deemed to be most important for their electromechanical responses.³⁰ Our results here re-emphasize the significance of such interactions, not only in the static or the quasi-static regime, but also in the dynamic regime at higher frequencies.

The current findings could be important for the design of new polymer ferroelectrics. It is quite remarkable that relaxor behavior in polymer ferroelectrics can be induced not only by chemical modification but also by microstructural modifications,⁴ and both such means could ultimately lead to a similar macroscopic response. The microstructural modifications during processing steps typically occur at length scales of several tens of nanometers. As we have shown here, short-range molecular dynamics, which occur at sub-nanometer length scales and are correlated to mainly crystal structure volumes, cannot therefore explain the role played by microstructure. Instead, the increased short-range molecular motion could play a facilitating role in switching of dipoles. However, the real significance of microstructure becomes apparent if one considers the interfacial effect which occurs between the amorphous and the crystalline domains. It is interesting that the coherent domain sizes in ceramic relaxor ferroelectrics is of the order of a few nanometers, while here in polymeric relaxor

ferroelectrics the coherent domain sizes are of the order of 25-30 nm. Therefore, further enhancement in the dielectric properties of polymer relaxor ferroelectrics could be possible by decreasing their domain sizes. However, the optimal limits of the crystalline domain sizes and the amorphous volume fractions needs to be determined, so that contributions from interactions at the crystalline-interface area can have a maximum effect on dielectric properties. Future materials design should focus on these aspects as well as fundamental physical phenomena at the interfacial region between crystalline and amorphous domains. The current study also establishes an experimental methodology to compare directly macroscopically measured dynamic response of a material with molecular dynamics. As demonstrated here, such a comparison could provide important insights into the microscopic origins of dynamic behavior of materials and therefore could lead to improved materials design.

SUPPLEMENTARY MATERIAL

See [supplementary material](#) for Details about measurement and analysis of dielectric permittivity, QENS, DSC thermograms, FTIR, X-ray diffraction and SAXS/SANS are provided.

ACKNOWLEDGMENTS

AP gratefully acknowledges funding support from CityU Start-up Grant for New Faculty (Project Number 7200514). The experiments conducted at the Spallation Neutron Source (SNS), High Flux Isotope Reactor (HFIR) and Center for Nanophase Materials Sciences (CNMS) in Oak Ridge National Laboratory was supported by the Scientific User Facilities Division, Office of Basis Energy Sciences, U. S. Department of Energy. STM thanks his Inamori Professorship which supported the HTXRD work at Alfred University. AP gratefully acknowledges technical assistance from Mr. Daniel Yau, Mr. Tak Fu Hung and Mr. Tit Wah Chan.

- ¹ E. Sun and W. Cao, "Relaxor-based ferroelectric single-crystals: Growth, domain engineering, characterization and applications," *Progress in Materials Science* **65**, 124 (2014).
- ² F. Bauer, "Review on the properties of the ferrorelaxor polymers and some new recent developments," *Appl. Phys. A* **107**, 567 (2012).
- ³ R. A. Cowley, S. N. Gvasaliya, S. G. Lushnikov, B. Roessli, and G. M. Rotaru, "Relaxing with relaxors: A review of relaxor ferroelectrics," *Advances in Physics* **60**, 229 (2011).
- ⁴ Q. M. Zhang, V. Bharti, and X. Zhao, "Giant electrostriction and relaxor ferroelectric behavior in electron-irradiated poly(vinylidene fluoride-trifluoroethylene) copolymer," *Science* **280**, 2101 (1998).
- ⁵ C. Ang and Z. Yu, "Ferroelectric, electroactive and dielectric-relaxation behavior of fluoropolymers," *Adv. Mater.* **16**, 979 (2004).
- ⁶ F. Bauer, "Relaxor fluorinated polymers: Novel applications and related developments," *IEEE Trans. Dielectric and Electrical Insulation* **17**, 1106 (2010).
- ⁷ J.-F. Capsal, E. Dantras, and C. Lacabanne, "Molecular mobility interpretation of the dielectric relaxor behavior in fluorinated copolymers and terpolymers," *Journal of Non-Crystalline Solids* **363**, 20 (2013).
- ⁸ C. Ang and Z. Yu, "Dielectric relaxor behavior of electroactive fluorinated polymers," *Appl. Phys. Lett.* **86**, 262903 (2005).
- ⁹ H.-M. Bao, J.-F. Song, J. Zhang, Q.-D. Shen, C.-Z. Yang, and Q. M. Zhang, "Phase transitions and ferroelectric relaxor behavior in P(VDF-TrFE-CFE) terpolymers," *Macromolecules* **40**, 2371 (2007).
- ¹⁰ V. Bharti and Q. M. Zhang, "Dielectric study of the relaxor ferroelectric poly(vinylidene fluoride-trifluoroethylene) copolymer system," *Phys. Rev. B* **63**, 184103 (2001).
- ¹¹ Y. Wang, S.-G. Lu, M. Lanagan, and Q. Zhang, "Dielectric relaxation of relaxor ferroelectric P(VDF-TrFE-CFE) terpolymer over broad frequency range," *IEEE Transactions on Ultrasonics, Ferroelectrics and Frequency Control* **56**, 444 (2009).
- ¹² R. Han, J. Jin, P. Khanchaitit, J. Wang, and Q. Wang, "Effect of crystal structure on polarization reversal and energy storage of ferroelectric poly(vinylidene fluoride-co-chlorotrifluoroethylene) thin films," *Polymer* **53**, 1277 (2012).
- ¹³ L. Yang, X. Li, E. Allahyarov, P. L. Taylor, Q. M. Zhang, and L. Zhu, "Novel polymer ferroelectric behavior via crystal isomorphism and the nanoconfinement effect," *Polymer* **54**, 1709 (2013).
- ¹⁴ G. Casar, X. Li, J. Koruza, Q. Zhang, and V. Bobnar, "Electrical and thermal properties of vinylidene fluoride-trifluoroethylene-based polymer system with co-existing ferroelectric and relaxor states," *J. Mater. Sci.* **48**, 7920 (2013).
- ¹⁵ M. R. Gadinski, Q. Li, G. Zhang, X. Zhang, and Q. Wang, "Understanding of relaxor ferroelectric behavior of poly(vinylidene fluoride-trifluoroethylene-chlorotrifluoroethylene) terpolymers," *Macromolecules* **48**, 2731 (2015).
- ¹⁶ H. Su, A. Strachan, and W. A. Goddard III, "Density functional theory and molecular dynamics studies of the energetics and kinetics of electroactive polymers: PVDF and P(VDF-TrFE)," *Phys. Rev. B* **70**, 064101 (2004).
- ¹⁷ E. Lopez Cabarcos, F. Batallan, B. Frick, T. A. Ezquerra, and F. J. Balta Calleja, "Molecular dynamics of ferroelectric polymer systems as studied by incoherent quasielastic neutron scattering," *Phys. Rev. B* **50**, 13214 (1994).
- ¹⁸ E. Lopez Cabarcos, A. F. Brana, B. Frick, and F. Batallan, "Thermal hysteresis loop in the elastic incoherent scattering function of vinylidene fluoride and trifluoroethylene ferroelectric copolymers," *Phys. Rev. B* **71**, 184304 (2005).

- ¹⁹ N. Jalarvo, A. Pramanick, C. Do, and S. O. Diallo, "Effects of configurational changes on molecular dynamics in poly(vinylidene fluoride) and poly(vinylidene fluoride-trifluoroethylene) ferroelectric polymers," *Appl. Phys. Lett.* **107**, 082907 (2015).
- ²⁰ E. Mamontov and K. W. Herwig, "A time-of-flight backscattering spectrometer at the Spallation Neutron Source, BASIS," *Rev. Sci. Instrum.* **82**, 085109 (2011).
- ²¹ O. Arnold, J. C. Bilheux, J. M. Borreguero, A. Buts, S. I. Campbell, L. Chapon, M. Doucet, N. Draper, R. Ferraz Leal, M. A. Gigg, V. E. Lynch, A. Markvardsen, D. J. Mikkelsen, R. L. Mikkelsen, R. Miller, K. Palmen, P. Parker, G. Passos, T. G. Perring, P. F. Peterson, S. Ren, M. A. Reuter, A. T. Savici, J. W. Taylor, R. J. Taylor, R. Tolchenov, W. Zhou, and J. Zikovsky, "Mantid—Data analysis and visualization package for neutron scattering and image μ SR experiments," *Nucl. Instrum. Methods Phys. Res., Sect. A* **764**, 156 (2014).
- ²² T. R. Azuah, L. R. Kneller, Y. M. Qiu, P. L. W. Tregenna-Piggott, C. M. Brown, J. R. D. Copley, and R. M. Dimeo, "DAVE: A comprehensive software suite for the reduction, visualization, and analysis of low energy neutron spectroscopic data," *J. Res. Natl. Inst. Stand. Technol.* **114**, 341 (2009).
- ²³ L. Yang, B. A. Yybarski, F. Dos Santos, M. K. Endoh, T. Koga, D. Huang, Y. Wang, and L. Zhu, "Relaxor ferroelectric behavior from strong physical pinning in a poly(vinylidene fluoride-co-trifluoroethylene-co-chlorotrifluoroethylene) random terpolymer," *Macromolecules* **47**, 8119 (2014).
- ²⁴ S. T. Lau, H. L. W. Chan, and C. L. Choy, "Structural and property changes in poly(vinylidene fluoride-trifluoroethylene) 70/30 mol % copolymer induced by proton irradiation," *Appl. Phys. A: Mater. Sci. Process.* **80**, 289 (2005).
- ²⁵ R. J. Klein, J. Runt, and Q. M. Zhang, "Influence of crystallization conditions on the microstructure and electromechanical properties of poly(vinylidene fluoride-trifluoroethylene-chlorofluoroethylene) terpolymers," *Macromolecules* **36**, 7220 (2003).
- ²⁶ K. Tashiro, K. Takano, M. Kobayashi, Y. Chatani, and H. Tadokoro, *Polymer* **25**, 195–208 (1984).
- ²⁷ H. Xu, Z.-Y. Cheng, D. Olson, T. Mai, Q. M. Zhang, and G. Kavarnos, "Ferroelectric and electromechanical properties of poly(vinylidene-fluoride-trifluoroethylene-chlorofluoroethylene) terpolymer," *Appl. Phys. Lett.* **78**, 2360 (2001).
- ²⁸ A. Pramanick, D. Damjanovic, J. E. Daniels, J. C. Nino, and J. L. Jones, "Origins of electro-mechanical coupling in polycrystalline ferroelectrics during subcoercive electrical loading," *J. Am. Ceram. Soc.* **94**, 293 (2011).
- ²⁹ D. Fu, H. Taniguchi, M. Itoh, S.-Y. Koshihara, N. Yamamoto, and S. Mori, "Relaxor $\text{Pb}(\text{Mg}_{1/3}\text{Nb}_{2/3})\text{O}_3$: A ferroelectric with multiple inhomogeneities," *Phys. Rev. Lett.* **103**, 207601 (2009).
- ³⁰ I. Katsouras, K. Asadi, M. Li, T. B. van Driel, K. S. Kjær, D. Zhao, T. Lenz, Y. Gu, P. W. M. Blom, D. Damjanovic, M. M. Nielsen, and D. M. de Leeuw, "The negative piezoelectric effect of the ferroelectric polymer poly(vinylidene fluoride)," *Nat. Mater.* **15**, 78 (2016).